

Utilising virtual prototyping technology to model and control the Mobile Harbour Crane System

Katthula Harinath Reddy, Prof Niranjana Kumar Injeti, Gorrela Solomonraju, Kelli Narsimha Naidu,
Maduthuri Venkatesh,
Research Scholar,
Department of Marine Engineering,
Andhra University,
Visakhapatnam , AP, INDIA.

Abstract: Utilising virtual simulation to replicate the actual performance of a mobile harbour crane (MHC) is a necessary strategy during the design phase. This method eliminates the need for the traditional trial-and-error process and can enhance the product's quality by minimising manufacturing expenses and faults. This paper introduces an engineering model that describes the mechanical behaviour of MHC, and the control design for increasing the position accuracy. A virtual mechanical model was generated using SOLIDWORKS based on the idea of the MHC. This model was subsequently transferred to the Automatic Dynamic Analysis of Mechanical System (ADAMS) environment. The purpose of this simulation was to analyse the dynamic functioning of the MHC system. Furthermore, a MATLAB/Simulink-based adaptive sliding mode PID controller was created to effectively regulate the position of the crane trolley and mitigate the oscillation of the load's swing angle. This co-simulation showcases the dependability of the mechanical and control features of the system that has been created.

Keywords: Adaptive sliding mode, mobile harbour crane, modeling and controlling, PID controller, virtual prototype.

1. INTRODUCTION

The fast expansion of the global economy has led to a significant increase in the need for goods transportation via huge container ships. Nevertheless, the present harbours have restricted capacity, preventing huge cargo ships from docking due to the shallow seas and small spaces. The option to increase the capacity of the ports is not possible owing to insufficient investment money and the adverse effects on environmental sustainability. In this context, a notion of MHC (Maximising the Utilisation of Containerships) was suggested[1]. This technique enables a container ship to anchor in deep water and efficiently load and unload containers. It also allows the ship to deliver the containers to their intended destination, regardless of the depth or narrowness of any ports. The MHC system, also known as a mobile harbour crane system, is a type of overhead crane system that is installed on a movable harbour. Its purpose is to facilitate the loading and unloading of containers between container ships and other vessels. The Mobile Harbour Crane (MHC) encounters greater difficulties compared to traditional ground-fixed cranes due to the challenging operating conditions. One significant issue is the oscillation of the

load due to inadequate trolley control and the impact of external disturbances, such as Oscillation and atmospheric movement.

This issue is of great concern since it has the potential to result in significant harm to nearby devices and systems. Moreover, when the container's swing reaches the conclusion of the transfer, it becomes challenging to precisely manage the container's intended location[2]. To enhance the productivity of the MHC system, it is necessary to ensure that all crane movements are performed at a high velocity and that the load is precisely regulated to achieve the required position. Nevertheless, meeting these criteria is challenging due to the undesirable swinging of the suspended weight as the tram undergoes acceleration or deceleration. In addition, the wind and wave disturbances from the outside, along with the constantly shifting base, result in an uncertain path for the load. Hence, achieving precise control over the load's location is a challenging problem to be resolved.

Typically, two mechanical and electrical methods have been suggested to counteract the swaying of the load.

The mechanical solution effectively mitigated the longitudinal wobble of the load in several testing scenarios. Nevertheless, this approach resulted in vibration, sluggish reaction time, and exorbitant maintenance expenses[3].

Fig.1.The mobile harbor crane system.



Typically, the electrical solution is commonly employed to counteract the swinging of the load. The solution was categorised into two types of control methods: open-loop control and closed-loop control. The open-loop control approach suggested in [4] did not have sensors incorporated. The control objectives were established using specified speed control and trajectory, which were simulated to eliminate the swing.

This approach is cost-effective and reliable when used with cranes that possess a low inherent frequency. Nevertheless, unstable plants, which are susceptible to perturbations, render the process ineffective. Subsequently, the closed-loop control systems were suggested as a means to counteract the swinging motion of the cranes. These systems are supplied with several types of sensors to monitor the angle of sway of the load in both linear and nonlinear controllers [5-11]. Before being communicated to the controller, the swing angle signal undergoes processing by observation and estimating models. Multiple devices were suggested to measure the angular displacement of the load. Yoshida et al. [10] suggested utilising cameras as a non-contact sensor to provide visual feedback control for the crane. For this particular situation, a 3D camera was mounted on the trolley to accurately determine the three-dimensional location of the load. This strategy is efficacious for cranes that encounter disruptions. Nevertheless, this visual system incurs high costs and presents challenges in terms of maintenance. Furthermore, the durability of vision equipment diminishes with time when they come into contact with the marine environment.

To substitute the view, [11] Proposed a novel sensor-less control method for container cranes, utilising an inclinometer mounted on the spreader to accurately measure the sway angle of the load. Nevertheless, conventional inclinometers suffer from a lack of high accuracy and have poor response times. Consequently, a costly inclinometer is required in order to get a high level of accuracy. In order to enhance efficiency, accuracy, and speed of reactions, Park et al. [12] proposed a novel method that utilised a tri-axial accelerometer to measure the swing. The swing angle is determined in this method by the accelerometer, which calculates the variation in fixed points between the trolley and the spreader. The aforementioned methods were employed in a collaborative manner with the objective of accurately detecting the swing angle and developing a closed-loop control system to successfully counteract the swinging motion of the load. These methods have successfully accomplished the intended control goals. Nevertheless, introducing and implementing a new control product in an actual work setting necessitates more resources in terms of time and expenses to construct, test, and validate on the physical prototype.

Therefore, this study suggests a virtual prototype simulation technique that combines ADAMS and MATLAB/Simulink. The ADAMS program is utilised for generating a virtual mechanical model, enabling the virtual measurement of various parameters for any components inside the virtual model. The MATLAB program is renowned for its ability to develop control systems. The co-simulation model we have developed for both software demonstrates a significant advantage in accurately mimicking the actual behaviour of the mechanical system.

prototype model. The simulations of results not only help designer to modify mechanical design but also improve the control method.

Where ρ = Air density,

C_D = Drag coefficient,

A = Projected area of a structure,

$U(t)$ = Incident wind speed,

Additionally, it effectively implements closed-loop control for the whole virtual system. demonstrates a significant advantage in accurately mimicking the actual behaviour of the mechanical system. Additionally, it effectively implements closed-loop control for the whole virtual system.

2. COMPOSITION AND WORKING PRINCIPLE OF THE MHC SYSTEM

The MHC is the crane system mounted on the floating as shown in Fig. 2. It consists of a floating, frame system, support frame, trolley, spreader and boom. The floating can carry whole crane systems and the load. It works on the sea and is swayed by the wind and wave. The frame system is a firm structure to withstand the total load of the crane. It moves along the floating and can be adjusted horizontally to pick up a container. The support frame is raised when the crane begins working and is lowered when stopped. This function aims to collapse the crane system for convenient traveling. The trolley moves on the boom rail following the x-direction and is driven by a motor force. It drives the spreader to the desired position to pick and insert a container. The spreader is suspended on the trolley by a four-cable mechanism, and its function is to adjust the hooks of a container for lifting. The clamping and positioning systems are used to locate the container accurately. Due to working on the sea, the MHC is influenced by the wind and wave. According to Jang et al. [14], the wind-induced drap force acting on the crane structures over the seaway can be evaluated based on the fundamental equation of drap force in aerodynamics:

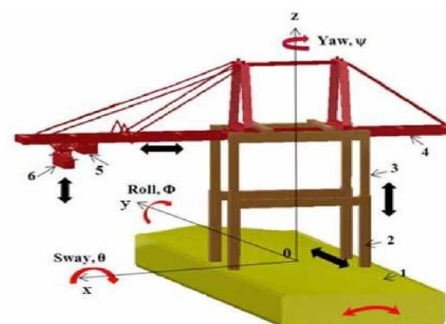
$$F_D(t) = \frac{1}{2} \rho C_D A U^2(t), \tag{1}$$

$$U(t) = U + w(t). \tag{2}$$

The \bar{U} is a constant wind speed depending on the height above the sea level, and the $w(t)$ is a randomly fluctuating turbulent wind speed. The wind-induced drag force, $F_D(t)$ can be written as follows:

1. Floating; 2. Frame; 3. Support frame; 4. Boom;
5. Trolley; 6. Spreader.

Fig.2. The MHC modeling.



$$F(t) = \frac{1}{2} \rho C A U^2 + \rho C A U w(t) + \frac{1}{2} \rho C A w(t) w(t) \quad (3)$$

The initial component of (3) is referred to be the average drag force, which remains consistent for a specific average wind speed. The forces associated with turbulent winds are represented by the second and third terms in equation (3). In the evaluation of wind-induced effects on structures, the third term in equation (3) is typically disregarded. The turbulent wind speed variation, denoted as $w(t)$, follows a Gaussian random process with a mean of zero. In this work, the MHC predicted area and height buildings are considered to be insignificant. Consequently, the impact of wind on the MHC structure is disregarded, and it is treated as a random Gaussian disturbance to the control system.

Alternatively, the floating motion is mostly affected by the disturbance created by sea waves. Understanding the phenomenon of excitation caused by sea waves is crucial for accurately modelling the floating system. In order to analyse the nonlinear system, the wave force is separated into two parts: the combination of a harmonic force at the main frequency and a minor random component [15].

The sea wave is represented by equation:

$$s_w(t) = f_a \sin(\Omega t + \Phi) + B \xi, \quad (4)$$

where the harmonic component of the force is denoted by $f_a \sin(\Omega t + \Phi)$, and the random disturbance by $B \xi$; f_a , Ω , and Φ are amplitude, frequency, and phase of wave, respectively.

According to Ngo et al. [9], the wave disturbance causes the MHC to undergo six degrees of freedom motions, which include three translational motions (surge, sway, and heave) and three rotational motions (roll, pitch, and yaw). The motion with six degrees of freedom is depicted in Figure 2. The literature examines traditional cranes that have coplanar trolley and sway actions for containers. The trolley motion is employed to mitigate the oscillation of the container. In the case of the MHC, the suspended load exhibits an extra lateral sway, which is caused by the pitch motion of the floating structure. The author presented a novel technique to regulate the lateral sway caused by a non-coplanar sway component in the trolley's movement direction.

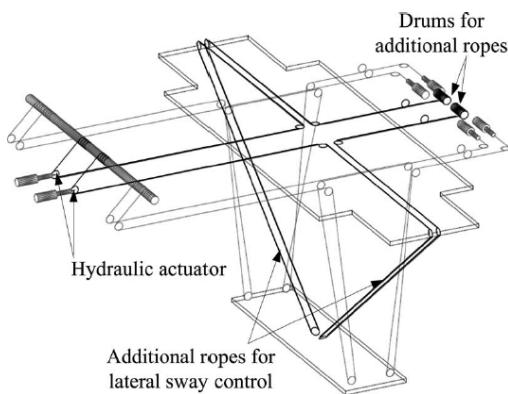


Fig.3. Proposed new mechanism for lateral sway control of load.

Fig.3 shows a new mechanism for lateral way Control of the load. The mechanism is equipped with Two extra ropes, along with the required pulleys and drums.

The drums are necessary to offset the disparities in rope length between the supplementary ropes and the primary hoist ropes during vertical movement of the container. Hydraulic actuators provide tension in the extra ropes, allowing for the imparting of a lateral-sway-suppressing force.

This research examines many assumptions related to the MHC system.

- 1) The buoyant object was intended to remain relatively stationary in the Cartesian coordinate system. Therefore, the movement of floating and the rotational motion in absolute coordinates may be disregarded.
- 2) The trolley's movement is analysed in the X-direction, together with the lateral movement of the load, which occurs on the same plane.
- 3) The oscillatory movements of the hanging load occurring on different planes might be regarded as disturbances to the control system.
- 4) The movement of the weight is analogous to a pendulum motion, and the friction force on the trolley is insignificant.

3. THE MHC SYSTEM MODELING

3.1. Importance of creating a virtual prototype for the MHC system
 Since the complexity of products has been increasing, in order to increase competition in production, the requirement of the product development cycle times should be reduced. Therefore, building a hardware prototype for testing has taken a majority of the time to launch a new product. The simulation technique based on the virtual prototype is proposed as an approach that significantly reduces manufacturing cost and time compared to the traditional build-and-test approach. The virtual prototyping approach is an integrating software solution that consists of modeling a mechanical system, simulating, and visualizing its 3D motion behaviour under real work operating conditions, and refining & optimising the design through iterative design studies [17]. The advantages of this simulation technique consist of conceiving a detailed model that is used in a virtual experiment in a similar way with a real scenario. The possibility to perform virtual measurements of any parameters and in any components of the mechanical model can also be carried out conveniently. Fig. 4 shows the creation of a virtual prototype for the testing of the MHC system.

In the design process of a mechatronic system, the mechanical design and control design stages are done separately with different software tools however the concept is the same. After the design, each separate model should be tested and verified for fulfilling the desired objectives, and finally a co-test should be implemented on the physical prototype to verify the proposed approaches. During testing on the physical prototype, if a problem appears in the interaction

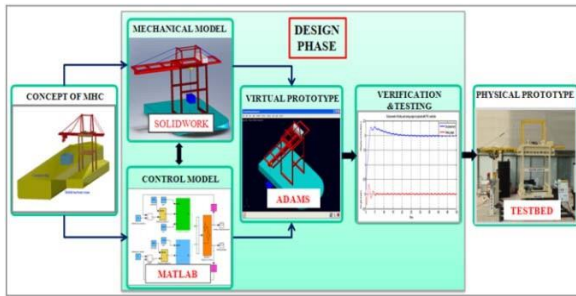


Fig.4.The creation of the virtual prototype model for testing of the MHC system.

operation between two systems, the designer must refine the mechanical design and/or the control design to achieve a perfect system. In this method, the physical testing process is more simplified. It saves time and cost and reduces the risk of device damage caused by the conflict between both systems.

2.1. The virtual prototyping platform

Fig. 5 shows a virtual prototyping platform which includes the following softwares: CAD-Computer Aided Design(SOLIDWORKS,CATIA,PROENGINEER); MBS-Multibody systems (ADAMS, SD-EXACT, PLEXUS); FEA- Finite Element Analysis (NASTRAN/ PATRAN, COSMOS, ANSYS) and Command &Control (MATLAB, EASY5, MATRIX) [17].

The CAD software is used to create the geometric model of the mechanical system. This model includes the rigid parts with shape and dimension of the physical prototype model, and it contains information about mass and inertia properties of these rigid parts. The CAD environment can perform simple motion testing with forces and torques. The geometry model is then exported from the CAD environment to the MBS environment using a file format as STEP (CATIA) or Parasolid. x_t (SOLIDWORKS). The MBS is the centre component of the virtual platform, and it is used for analysing, optimising, and simulating the kinematic and dynamic behaviour of the mechanical system under real operating conditions. The FEA software is used for modeling flexible components. The MBS has an ability to transfer loads to FEA and receive the flexible components feedback from FEA. This feature enables the capturing of inertia and compliance effects, and predicting loads with greater accuracy, hence obtaining more realistic results. Command & Control (C&C) is a software product which is used to design the control system. This software exchanges information with the MBS software. The exchange process creates a closed loop in which the outputs from the MBS model are the inputs for the control system and vice-versa. The outputs from MBS

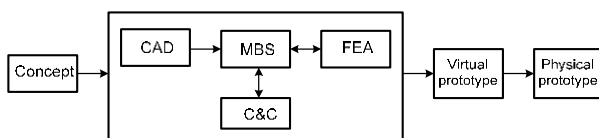


Fig.5.The virtual prototyping platform.

model are measured parameters that are necessary for control, and the outputs from control system effect on the MBS simulation.

2.2. Modeling a MHC mechanical system

To create the mechanical model of the MHC system, any components or pieces that have the same shape and dimensions as the physical model are represented as 3D solids using SOLIDWORKS. The geometric limitations were utilised to build these components, which exhibit the properties of the MHC system. The mechanical model was used to assess the actual behaviour by applying torque and force to drive the components of the MHC model. Subsequently, it was exported to ADAMS in order to carry out the dynamic simulation. A MHC modelling is produced in the ADAMS/view environment. The modelling method is structured as a sequential sequence to provide easy modifications throughout the design phase. Initially, it is necessary to establish the geometrical characteristics of the components, including their material, mass, and density. Subsequently, the mass and inertial matrices are automatically constructed. These sections are interconnected to the floating coordinate using the following geometric restrictions, accordingly. The following text provides a description of these restrictions. The floating mass coordinate's centre (referred to as 1) is rigidly attached to the centre of the Cartesian coordinate in ADAMS via a revolute joint. The floating motion is influenced by the wave disturbance function. The frame, indicated as 2, is affixed to the floating object and is capable of being moved along the floating object by means of a translational joint. The trolley, represented by the symbol 3, is propelled by a motor-generated force and moves along the x-axis on the frame via a translational joint. The container (shown by 4) is connected to the trolley using a spherical joint and is thereafter moved in accordance with the trolley's movement. Figure 6 depicts the virtual prototyping of the mechanical model of the MHC system. The virtual prototype model is used to simulate and study the actual behaviour of the mechanical MHC model. The parameter settings utilised in the Adams simulation are displayed in Table 1. The computer simulation results of the ADAMS model will be examined and verified against the experimental data obtained from the test bed in order to assess the precision of the ADAMS model. Figures 7 and 8 display the comparison between the simulated and experimental findings of the trolley displacement and the sway angle of the load, respectively. By making these comparisons, we can assess that the curves of both simulation and experiment are in excellent agreement.

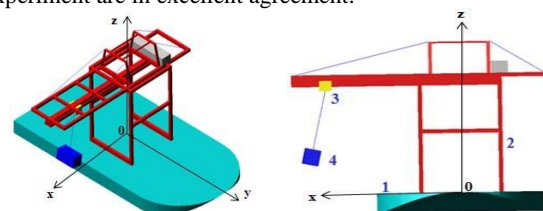


Fig.6. The Adams model of the MHC system.

Table1.The parameter values used in the simulation.

Parameters	Values
Simulation time	t =50 sec
The trolley trajectory: - Translation follows the x-axis - Translation follows the y-axis	$x=\text{step}(\text{time},0,0,30,3.8)$ $y=\text{step}(\text{time},30,0,50,3)$
Crane height	h = 3m
Rope length	l =1.2m
Trolley mass	m= 127kg
Container mass	m= 148kg
Wave disturbance function	$S_w(t)=0.02\sin(1.5\text{time})\text{rad}$

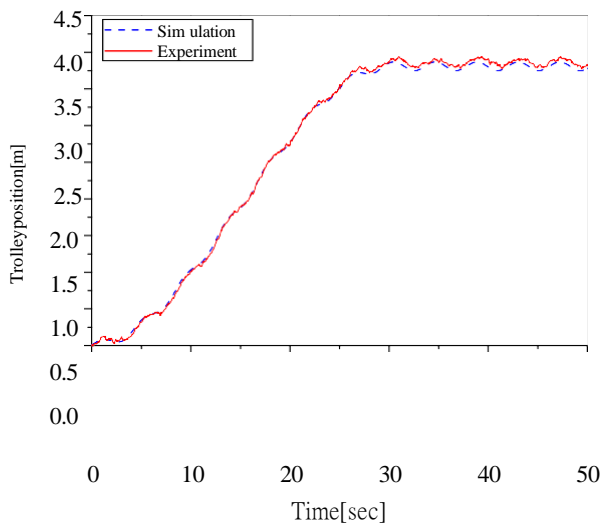


Fig.7.The comparison between simulation and experiment responses of the trolley displacement.

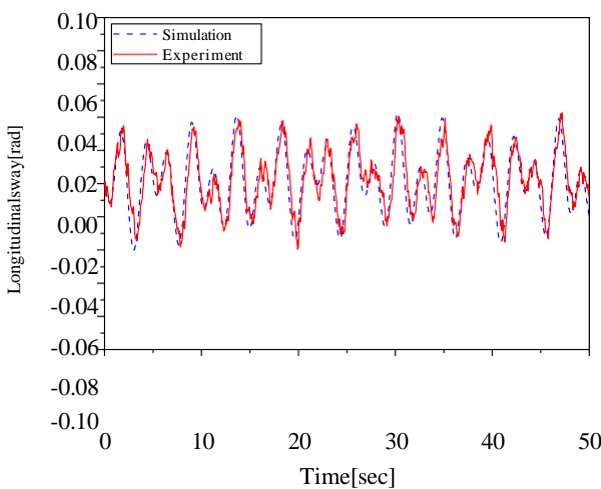


Fig.8.The comparison between simulation and experiment responses of the sway angle of load.

2.3. Hence, the ADAMS model may be employed to replicate the attributes of the MHC mechanical model. This model may also be utilised to simulate, study, test, and validate the behaviour of both the mechanical and control systems.

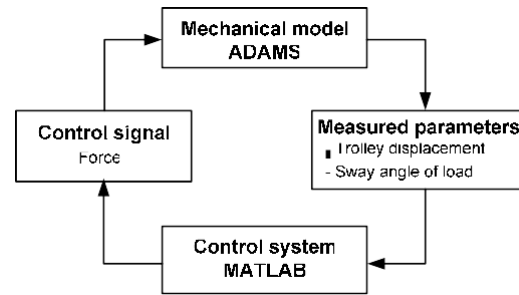
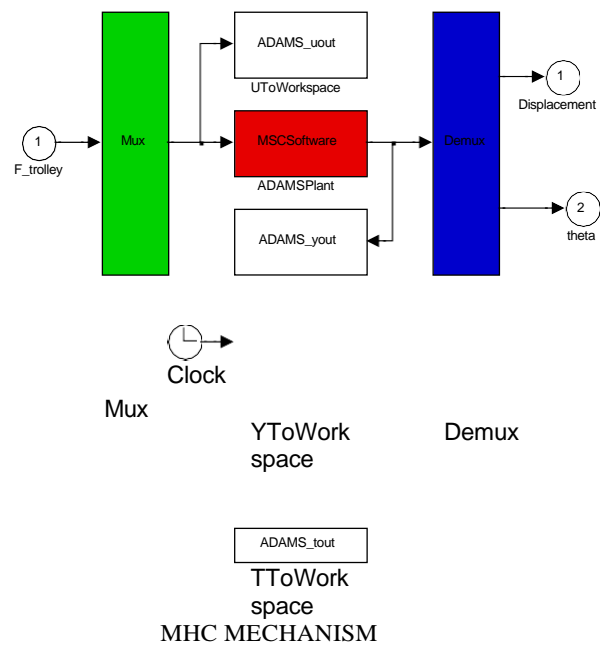


Fig.9.The connection of Adams and Matlab in the co-simulation model.



3.1. Generating an adams_sys in MATLAB/Simulink It is essential to create a control system for the virtual MHC model in order to combine the two different simulation programs into a unified system through co-simulation. The control design is formulated using ADAMS/Control and MATLAB/Simulink. In order to transfer the virtual MHC mechanical model from ADAMS to the MATLAB environment, the input and output variables are initially specified within the ADAMS model.

Fig.10.The ADAMS block in adams_sys.

The input signal serves as the governing force for the movement of the tram. The output signals correspond to the measured parameters of the trolley location and the swing angle of the load, respectively. Afterwards, this model is exported to MATLAB/Simulink. Figure 9 illustrates the linkage between Adams and Matlab in the co-simulation model.

Within the MATLAB environment, a .m file and an adams_sys are generated. The adams_sys showcases the non-linear MSC.ADAMS model, namely the MHC mechanical system, as seen in Figure 10. The ADAMS block is generated using the data provided by the .m file [17]. The adams_sys function is utilised to construct a control system in MATLAB/Simulink. The input signal is the signal generated by the controller, while the output signals are the measured values of the trolley displacement and the swing angle of the load, respectively.

3.1. Controllerdesign

The MHC model is a nonlinear system that operates in hostile conditions, experiencing external disturbances and fluctuations in system parameters. In this scenario, the conventional PID controller, which consists of three PID gains (proportional gain K_P , integral gain K_I , and derivative gain K_D), cannot be utilised to regulate the position and angle of the MHC system. This work introduces an adaptive sliding mode PID controller (ASMP) as a means to enhance system robustness against parameter fluctuations. The ASMP controller combines the benefits of PID and sliding mode controllers [18]. Figure 11 depicts the block diagram of the adaptive sliding mode PID control system designed for the MHC.

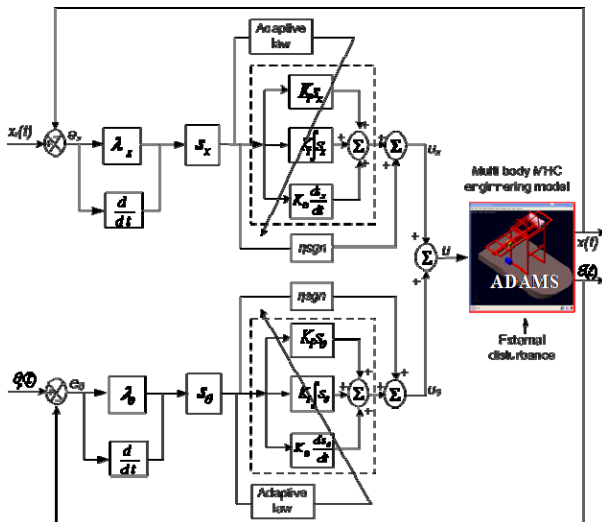


Fig.11. Block diagram of adaptive sliding mode PID control system for the MHC.

Previous studies have utilised the sliding mode controller approach to address uncertainty in the system [9,16,24]. Sliding mode control (SMC) is a contemporary control technique that use a state-space approach to examine systems of this nature. SMC has the benefit of being resistant to changes in system parameters and external disturbances. SMC addresses uncertainty by guiding the plant's state trajectory onto a sliding surface and ensuring that the error trajectory remains on this surface for all future times. The sliding surface is constructed in such a way that the state tracking error approaches zero as the input reference is applied [24]. A novel adaptive rule is devised to enable online updating of the PID control gains. This adaptation process is designed to be responsive to variations in system parameters and external disturbances.

This research examines the MHC system as a single-input and multi-output nonlinear system, based on the nonlinear systems specified in Wang's study [16]. It assumes that the trolley motion is along the X-direction, and expresses the couple systems in the following form:

$$\begin{aligned}
 \dot{x}_1 &= x_2, \\
 \dot{x}_2 &= f_1(X) + b_1(X)u_x + d_1(t), \\
 \dot{x}_3 &= x_4, \\
 \dot{x}_4 &= f_2(X) + b_2(X)u_\theta + d_2(t),
 \end{aligned} \tag{5}$$

where $X = (x_1, x_2, x_3, x_4)$ is state variables vector that represents the position and velocity of trolley, the sway angle and angle velocity of pay load. The $f_1(X), f_2(x), b_1(X)$ and $b_2(X)$ are the nonlinear functions. The $d_1(t)$ and $d_2(t)$ are the bounded lumped disturbances which include the system parameter variations and external disturbances (i.e., they satisfy $|d_1(t)| \leq d_{1M}$ and $|d_2(t)| \leq d_{2M}$, where d_{1M}, d_{2M} are known non negative constants), And u is the control input to control the crane trolley Position and sway angle of pay load to achieve the desired objectives.

From (5), the MHC system has two subsystems: the positioning subsystem of the crane trolley, and the anti-swing of payload. The sliding surfaces of the two subsystems are defined as:

$$\begin{aligned}
 s_x &= \dot{x} + \lambda_x e_x, \\
 s_\theta &= \dot{\theta} + \lambda_\theta e_\theta.
 \end{aligned} \tag{6}$$

In this work, a control input u was designed to control the trolley position and suppress the swing angle of the load simultaneously. The design methods for these two controllers are similar, hence the method for designing the trolley position controller is presented.

The sliding surface of the trolley position controller is rewritten as.

$$s_x = \dot{x} + \lambda_x e_x, \tag{7}$$

where $e_x = x_d - x$, x_d is the desired position; x is the measured position; and λ_x is a positive constant.

Derivating (7)

$$\dot{s}_x = \ddot{x} + \lambda_x \dot{e}_x = \dot{x}'_d - \dot{x}' + \lambda_x \dot{e}_x \tag{8}$$

Substituting $\dot{x}'_d = \dot{x}'$ from (5) into (8), we have

$$\dot{s}_x = \dot{x}'_d - f_1(X) - b_1(X)u_x - d_1(t) + \lambda_x \dot{e}_x \tag{9}$$

The control input u of PID controller is designed based on (9)

$$u_{PID} = \frac{1}{b_1(X)} [\dot{x}'_d - f_1(X) - d_1(t) + \lambda_x \dot{e}_x] = AB + \varepsilon, \tag{10}$$

where $A = [K_P \quad K_I \quad K_D]$; vector of the gain of PID

controller; $B = \begin{bmatrix} \dot{x}'_d \\ s_x \\ \frac{ds_x}{dt} \end{bmatrix}$ basic vector of PID controller; ε is an approximate error.

The control signal u_x of the position controller is determined as:

$$u_x = u_{PID} + u_h = \hat{A}B + u_h, \tag{11}$$

where \hat{A} is estimated value of vector $A, \hat{A} = [K_P \quad K_I \quad K_D]$; u_h is control signal of the auxiliary controller.

Substituting (11) into (9) yields:

$$\begin{aligned}
 \dot{s}_x &= \dot{x}'_d - f_1 - b_1 [\hat{A}B + u_h] + \lambda_x \dot{e}_x \\
 &= b_1 \tilde{A}B + b_1 \varepsilon - b_1 u_h,
 \end{aligned} \tag{12}$$

where $\tilde{A} = A - \hat{A}$ is estimation error.

In order to prove the stability, the Lyapunov function can be used.

$$V = \frac{1}{2} s^2 + \frac{1}{2\gamma} \tilde{A}^2 \tag{13}$$

Derivating (13) yields:

$$\begin{aligned} \dot{V} &= s_x \dot{s}_x + \frac{1}{\gamma} \ddot{\Delta} \\ &= s_x (b_1 \ddot{\Delta} + b_1 \varepsilon - b_1 u_h) + \frac{1}{\gamma} \ddot{\Delta} \\ &= \left(s_x b_1 + \frac{1}{\gamma} \right) \ddot{\Delta} + s_x \varepsilon - s_x u_h \end{aligned} \quad (14)$$

$$\begin{pmatrix} s_x b_1 + \frac{1}{\gamma} & 0 \\ 0 & -A \end{pmatrix} \neq 0 \quad (15)$$

Hence, $A = -A = -\gamma s_x b_1 B$.

The three PID controller gains including K_p, K_i , and K_D are on-line updated by the following adaptive laws

$$\begin{aligned} \dot{K}_p &= \gamma s_x b_1 s_x \\ \dot{K}_i &= \gamma s_x b_1 \int s_x \\ \dot{K}_D &= \gamma s b \frac{ds_x}{dt} \end{aligned} \quad (16)$$

Considering (14)

$$\begin{aligned} \dot{V} &= b \varepsilon s_x - b \eta \text{sgn}(s_x) s_x \\ &= b_1 \varepsilon s_x - b_1 \eta |s_x| < b_1 |s_x| (\varepsilon - \eta) < 0 \\ \Rightarrow \eta &> \varepsilon, \end{aligned} \quad (17)$$

where $u_h = \eta \text{sgn}(s_x)$ is the sign function.

$$\text{sgn}(s_x) = \begin{cases} 1 & \text{if } s_x > 0 \\ 0 & \text{if } s_x = 0 \\ -1 & \text{if } s_x < 0 \end{cases} \quad (18)$$

Equation (14) proves that the sliding surface is stability.

The control input for controlling the MHC model is composed of the trolley position control input u_x and the angle control input u_θ as:

$$u = u_x + u_\theta \quad (19)$$

4. SIMULATION RESULTS

The simulation is conducted in the MHC virtual model, taking into account wave disturbance and fluctuations in system parameters. The wave disturbances are altered by the amplitude and frequency of the oceanic wave. Meanwhile, the system characteristics, such as the load and strain of the rope, are altered by the length and mass. The simulation parameters are provided in Table 2.

The requirements for the control goals of the ASMP controllers, as outlined by Solihin et al. [19], include tracking the location of the trolley and suppressing the sway angle of the load.

This optimisation takes into account the following desirable specifications:

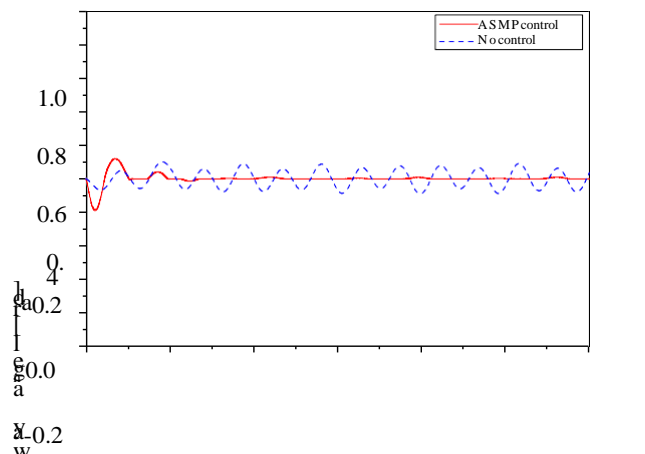
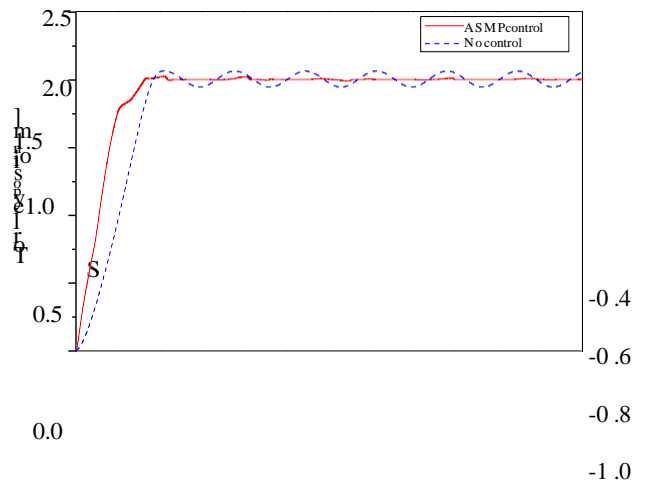
- Overshoot $\leq 2\%$
- Settling time $\leq 5s$
- Steady state error $\leq \pm 15\%$.

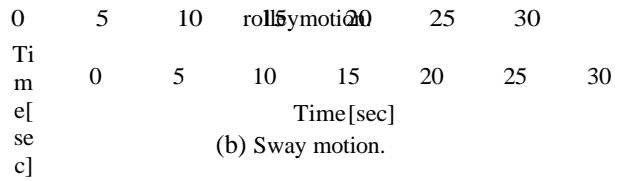
On the other hand, in order to suppress the swing angle quickly, the ASMP controller is optimised based on the following desired specifications:

- Settling time $\leq 5s$
- Residual swing $\leq \pm 0.05$ rad.

Table 2. The system parameters for simulation.

Parameters	Values
Simulation time (t)	30sec
The control objectives:	
- Desired trolley position (X_d)	2.0m
- Desired sway angle of load (θ_d)	0 rad
Model parameters:	
- Crane height (h)	3 m
- Rope length (l)	1.2m; 1.5m
- Trolley mass (m_t)	127 kg
- Load mass (m_l)	148 kg; 350kg
Disturbance parameters:	
- Sea wave height (h_w)	0.02m; 0.04m
- Sea wave frequency (f_w)	1.5rad/sec; 3 rad/sec
Control gains of the ASMP:	$\lambda=200, \gamma=1e-15,$
- Tracking the desired position	$b=1/127, \lambda=200,$
- Tracking the desired angle	$\gamma=1e-9, b=1$

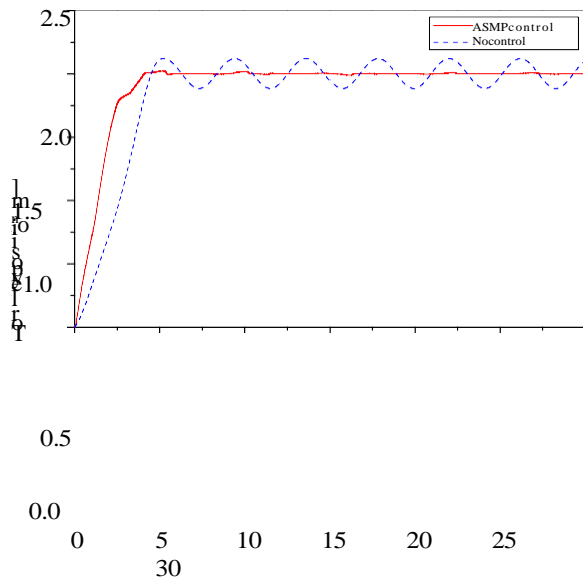




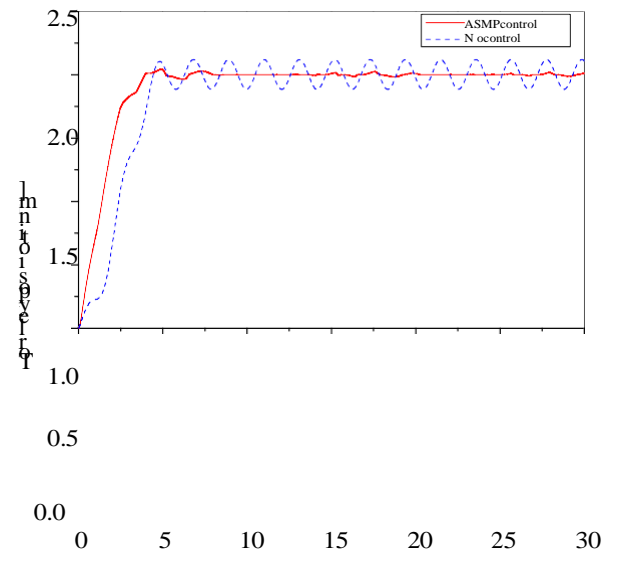
(a) Trolley position response

Fig.12. The position and angle responses of ASMP control with $h_w = 0.02$ m, $f_w = 1.5$ rad/s, $l = 1.2$ m, $m = 148$ kg.

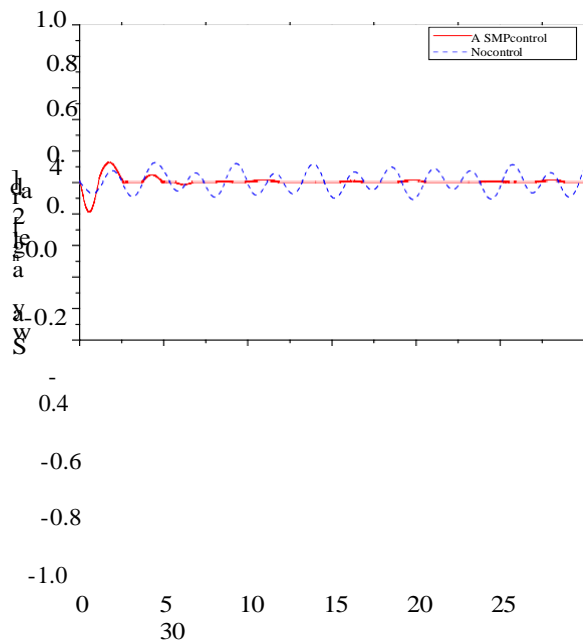
The ASMP controller for the trolley position is designed to provide fast movements with little overshoot.



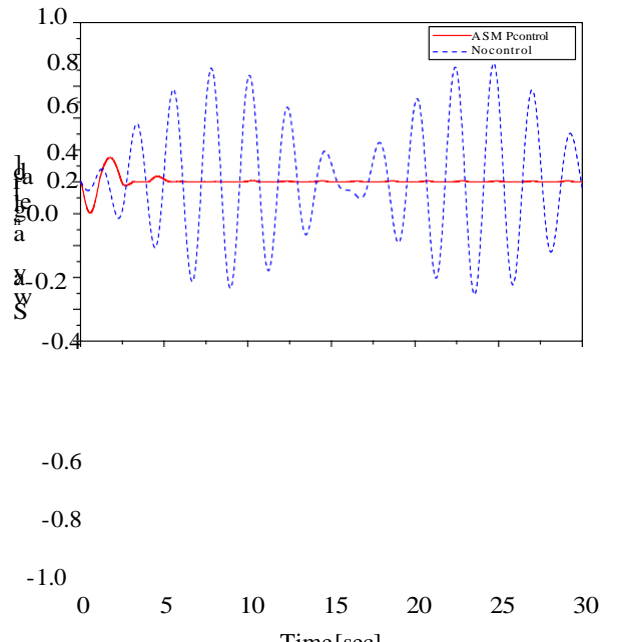
(a) Trolley motion.



(a) Trolley motion.



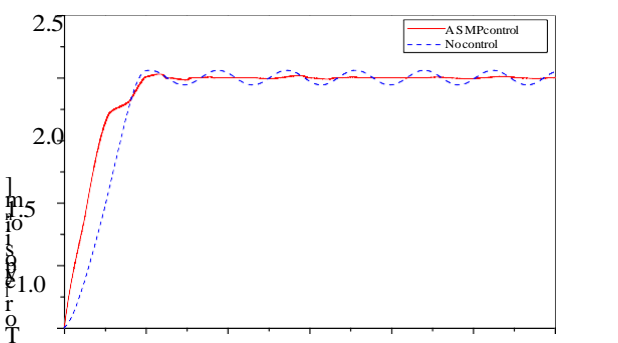
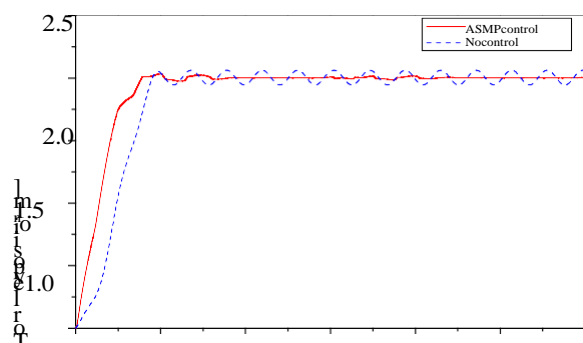
(b) Sway motion.



(b) Sway motion.

Fig.13. The position and angle responses of ASMP control with $h_w = 0.04$ m, $f_w = 1.5$ rad/s, $l = 1.2$ m, $m_l = 148$ kg.

Fig.15. The position and angle responses of ASMP control with $h_w = 0.04$ m, $f_w = 3$ rad/s, $l = 1.2$ m, $m_l = 148$ kg.



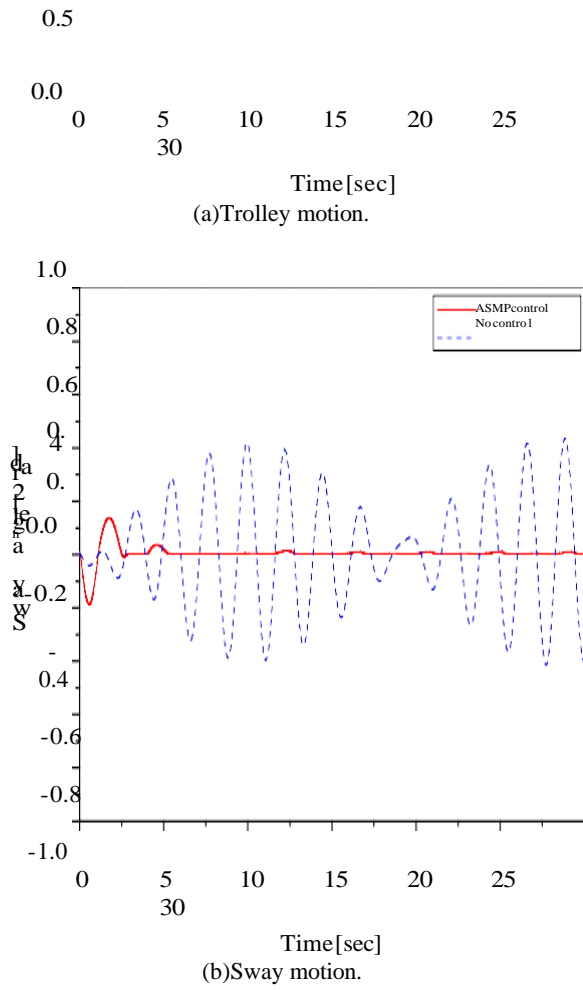


Fig.14. The position and angle responses of ASMP control with $h_w = 0.02$ m, $f_w = 3$ rad/s, $l = 1.2$ m, $m_l = 148$ kg.

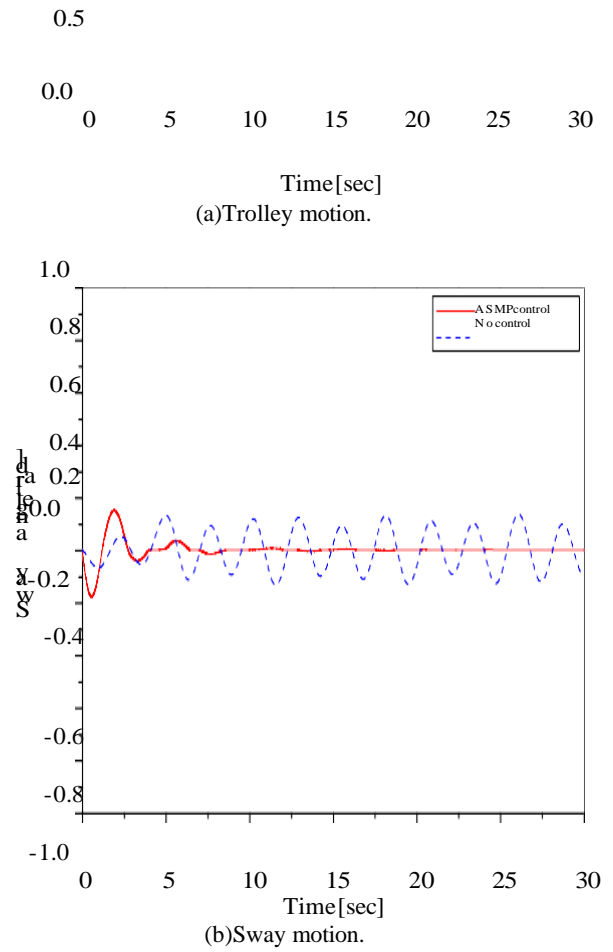
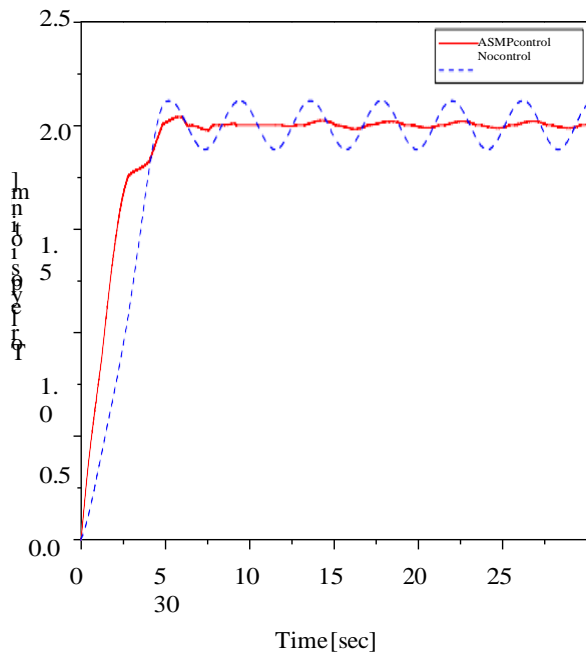
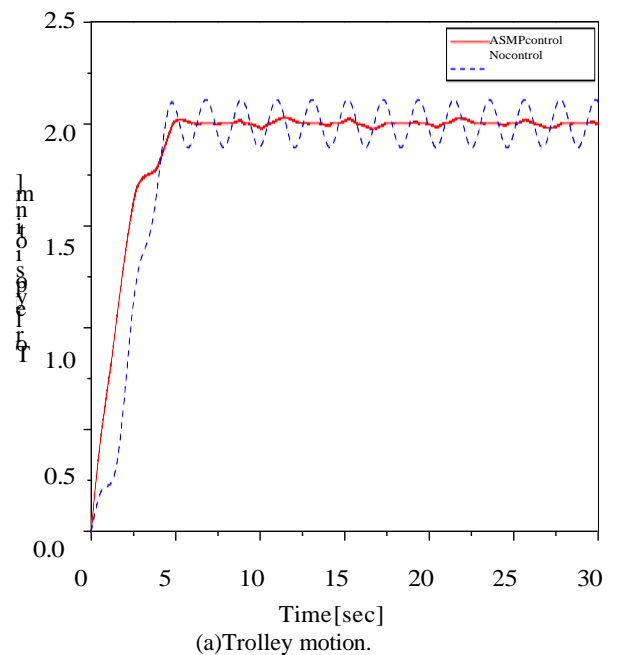


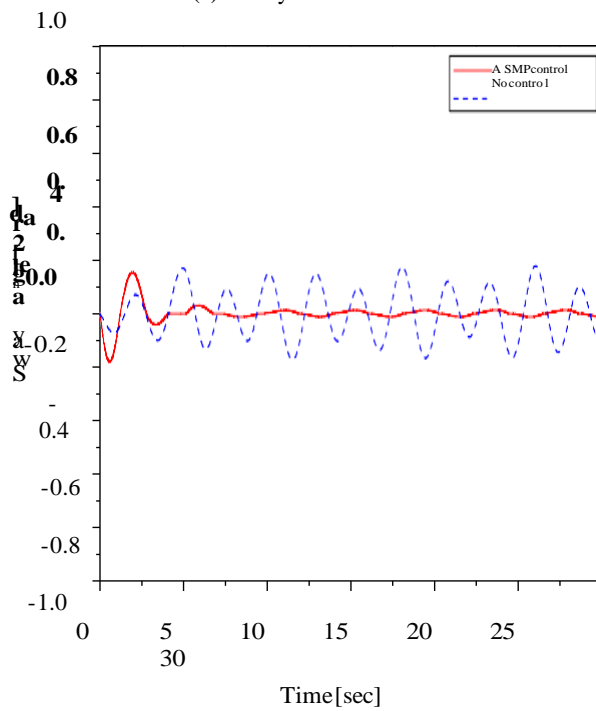
Fig.16. The position and angle responses of ASMP control with $h_w = 0.02$ m, $f_w = 1.5$ rad/s, $l = 1.5$ m, $m_l = 350$ kg.



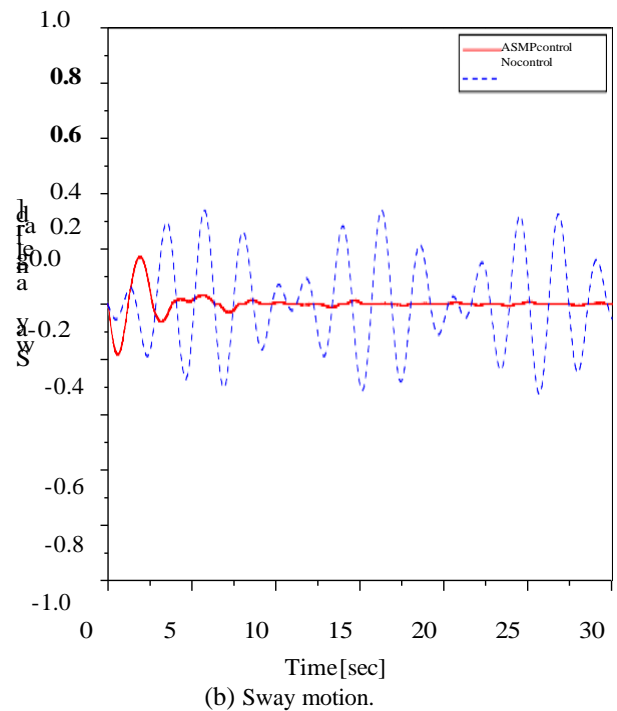
(a) Trolley motion.



(a) Trolley motion.



(b) Sway motion.



(b) Sway motion.

Fig.17. The position and angle responses of ASMP control with $h_w=0.04$ m, $f_w=1.5$ rad/s, $l=1.5$ m, $m=350$ kg.

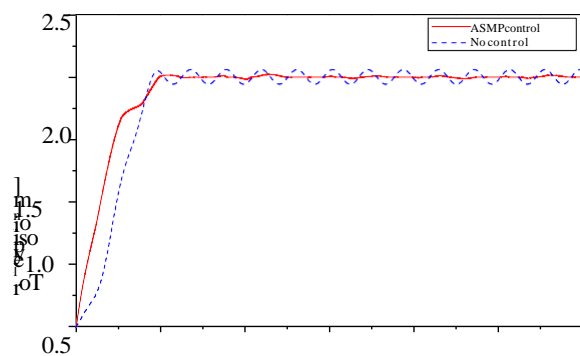


Table4. Comparison of anti-swing performances.

Simulation Performance	Fig. 12(b)	Fig. 13(b)	Fig. 14(b)	Fig. 15(b)
Nocontrol harmonicoscillation withamplitude(rad)	0.1	0.12	0.43	0.75
ASMPcontroller				
Amplitude (rad)	0.12	0.12	0.13	0.14
Settlingtime(s)	2.6	2.6	2.6	2.6

Table5. Comparison of positioning performance.

Simulation Performance	Fig. 16(a)	Fig. 17(a)	Fig. 18(a)	Fig. 19(a)
Nocontrol harmonicoscillation with amplitude (m)	0.06	0.12	0.06	0.12
ASMPcontroller				
Overshoot (%)	1.4	1.8	1.1	1.5
Settling time (s)	5	5	5	5
Error(m)	0	0	0	0

Table6. Comparison of anti-swing performance.

Disturbance Performance	Fig. 16(b)	Fig. 17(b)	Fig. 18(b)	Fig. 19(b)
Nocontrol harmonicoscillation withamplitude(rad)	0.14	0.18	0.20	0.34
ASMPcontroller				
Amplitude (rad)	0.13	0.15	0.15	0.16
Settlingtime(s)	3.8	3.8	3.8	3.8

The positioning response accurately follows the required position, effectively eliminating any longitudinal sway component. Thus, it can be inferred that the suggested ASMP control method may be efficiently employed in the MHC system to accurately regulate the trolley position and mitigate the swing angle of the load.

Overall, the analysis of all simulation examples demonstrates that the proposed ASMP controller is resilient to changes in system parameters and disturbances.

5. CONCLUSION

This research presents the simulation of the dynamic behaviour of the MHC system using ADAMS. The test was conducted to validate the mechanical performance of the MHC system in the virtual model, aligning with the physical mechanical system. A co-simulation model of the MHC control system, utilising the ASMP control technique, was created using ADAMS and MATLAB/ Simulink. The purpose of this model was to analyse the performance of the ASMP controller under conditions of disturbance and fluctuations in system parameters. The simulation findings demonstrate that the ASMP controllers exhibit robustness in the face of disturbances and fluctuations in system parameters.

Figure 20 displays the UOU test bed, which was fabricated at the University of Ulsan in Korea. The validation of the proposed ASMP approach will be conducted on this test bed, and the findings of the experimental investigation will be provided in a forth coming article. The dynamic mechanical behaviour of the MHC system may be analysed and evaluated using a co-simulation method that replaces the traditional build-and-test methodology.



Fig.20.TheMHCtestbedatUniversityofUlsan. Table 7.

Parameters of prototype UOU crane.

Parameter	Value
Base length	2.0m
Width	1.2m
Height	3.2m
Boom length	5.1m
Total weight	700kg

This method use commercial software. This method can significantly assist designers in modifying mechanical and control systems to remove mistakes and enhance accuracy.

REFERENCES

- [1] H. S. Park, D. B. H. Anh, and L. C. Hieu, "Computer based generation of control programs for a high speed mobile harbour crane in a novel maritime container handling system," *Proc. of Iproms Conference of Production Automation and Control*, Korea, November 2010.
- [2] A. Z. Al-Garni, K. A. F. Moustafa, and S. S. A. K. Javeed Nizami, "Optimal control of overhead cranes," *Control Eng. Practice*, vol. 3, no. 9, pp. 1277-1284, 1995.
- [3] Y. S. Kim, H. S. Seo, and S. K. Sul, "A new anti-sway control scheme for trolley crane system," *Proc. of Industry Applications Conference of Thirty-sixth IAS Annual Meeting*, vol. 1, pp. 548-552, Korea, September 2001.
- [4] K. T. Hong, C. D. Huh, and K. S. Hong, "Command shaping control for limiting the transient sway angle of crane systems," *International Journal of Control, Automation, and Systems*, vol. 1, no. 1, pp. 43-53, 2003.
- [5] Y. S. Kim, K. S. Hong, and S. K. Sul, "Anti-sway control of container cranes: inclinometer, observer, and state feedback," *International Journal of Control, Automation, and Systems*, vol. 2, no. 4, pp. 435-449, 2004.
- [6] Y. Fang, W. E. Dixon, D. M. Dawson, and E. Zergeroglu, "Nonlinear coupling control laws for an underactuated overhead crane system," *IEEE/ASME Trans. on Mechatronics*, vol. 8, no. 3, pp. 418-423,

- September 2003.
- [7] H. Kawai, Y. B. Kim, and Y. W. Choi, "Anti-sway system with image sensor for container cranes," *J. Mech.Sci.Technol.*, vol.23,no.10,pp.2757-2765, 2009.
- [8] H. Park, D. Chwa, and K.-S. Hong, "A feedback linearization control of container cranes: varying rope length," *International Journal of Control, Automation, and Systems*, vol.5,no.4,pp.379-387, 2007.
- [9] Q. H. Ngo and K. S. Hong, "Sliding mode antisway control of an offshore container crane," *IEEE/ASME Trans.onMechatronics*, vol.17,no. 2,pp.201-209, April 2012.
- [10] Y. Yoshida and H. Tabata, "Visual feedback control of an overhead crane and its combination with time-optimal control," *Proc. of IEEE/ASME International Conference Advanced Intelligent Mechatronics*, pp. 1114-1119, July 2008.
- [11] Y.S.Kim, H. Yoshihara, N. Fujioka, H. Kasahara, H. Shim, and S. K. Sul, "A new vision-sensorless anti-sway control system for container cranes," *Proc. of Industry Applications Conference of 38th IAS Annual Meeting*, vol. 1, pp. 262-269, October 2003.
- [12] K. R. Park and D. S. Kwon, "Swing-free control of mobile harbour crane with accelerometer feedback," *Proc. of International Conference on Control, Automation and Systems*, pp. 1322-1327, Oct. 2010.
- [13] Q.H.Ngo, K.S.Hong, K.H.Kim, Y.J.Shin, and S. H. Choi, "Skew control of a container crane," *Proc. of International Conference on Control, Automation and Systems*, pp.1490-1494, Oct.2008.
- [14] J. J. Jang and G. J. Shinn, "Analysis of maximum wind force for offshore structure design," *Journal of Marine Science and Technology*, vol.7,no.1,pp. 43-51, 1999.
- [15] P. T. D. Spanos, "Filter approaches to wave kinematics approximations," *Journal of Applied Ocean Research*, vol. 8, no. 1, pp. 2-7, Jan. 1986.
- [16] W. Wang, J. Yi, D. Zhao, and D. Liu, "Design of a stable sliding-mode controller for a class of second-order underactuated systems," *IEE Proc.-Control Theory Appl.*, vol.151,no.6,pp.683-690, Nov. 2004.
- [17] C. Alexandru and C. Pozna, "Dynamic modeling and control of the windshield wiper mechanisms," *Journal WSEAS Transaction on Systems*, vol.8,no. 7, pp. 825-834, July 2009.
- [18] T. C. Kuo, Y. J. Huang, C. Y. Chen, and C. H. Chang, "Adaptive sliding mode control with PID tuning for uncertain systems," *Engineering Letters*, vol. 16, no. 3, pp. 311-315, 2008.
- [19] M. I. Solihin and Wahyudi, "Sensorless anti-swing control for automatic gantry crane system: model-based approach," *International Journal of Applied Engineering Research*, vol.2,no.1,pp.147-161, 2007.
- [20] D.G.Ullman, *The Mechanical Design Process*, McGraw-Hill, Columbus, 1997.
- [21] W. Guojun, X. Linhong, H. Fulun, and Z. Xia, *Intelligent Systems and Applications*, ISA, 2009.
- [22] S. Jung, H.-T. Cho, and T. C. Hsia, "Neural network control for position tracking of a two-axis inverted pendulum system: experimental studies," *IEEE Trans.on Neural Networks*, vol.18,no.4,pp. 1042-1048, July 2007.
- [23] Y. Liu and Y. Li, "Dynamic modeling and adaptive neural-fuzzy control for nonholonomic mobile manipulators moving on a slope," *International Journal of Control, Automation and Systems*, vol. 4, no. 2, pp. 197-203, April 2006.
- [24] A. N. K. Nasir, R. M. T. Raja Ismail, and M. A. Ahmad, "Performance comparison between sliding mode control (SMC) and PD-PID controllers for a nonlinear inverted pendulum system," *World Academy of Science, Engineering and Technology*, vol. 70, pp. 400-405, 2010.